

Photogrammetry-based 3D digitization Method for Oil Paintings

CHEN Chen ; State Key Laboratory of Pulp and Paper Engineering, South China University of Technology, Guangzhou, Guangdong province 510640, China; Shen Zhen Polytechnic; Shen Zhen, Guangdong province 518055, China

WANG Xiaochun ; State Key Laboratory of Pulp and Paper Engineering, South China University of Technology, Guangzhou, Guangdong province 510640, China

CHEN Guangxue ; State Key Laboratory of Pulp and Paper Engineering, South China University of Technology, Guangzhou, Guangdong province 510640, China

Abstract

This paper proposes a new oil painting digitization method using photogrammetry technology to compensate for the deficiencies of the existing methods. The color and the 3D geometric information of the oil painting are recovered better by acquiring several sets of orthophotomaps, and modeling accuracy is ensured with a control mesh or by flattening. The 3D reconstruction and digital representation of oil paintings mainly includes two aspects: 3D geometric information recovery of oil painting surface and color rendition of oil painting. Photogrammetry can acquire a digital 3D model of the surface geometrics of an oil painting, restore the color image and plane geometry of the painting in the form of orthophotomap, and implement the 3D digital representation of color in the painting.

Keywords : 3D digitization method for oil paintings, photogrammetry, 3D modelling

1. Introduction

Oil paintings are reproduced primarily for decoration, promotion, dissemination, and reference. Reproductions have high value and great market demand, especially because the originals are difficult for ordinary consumers and art learners to obtain. High-fidelity reproductions are becoming increasingly popular. Currently, high-fidelity reproduction of oil paintings is achieved mainly through two methods, namely, manual copying and printing. Manual copying with oil paints often produces real and stereoscopic perception and feel. However, this process is time consuming, and the painting quality largely depends on the artist's painting skill. The following three printing methods exist:

- 1) Offset printing and digital inkjet printing (Wenhua Lian, 2007)¹;
- 2) Screen printing (Anning Liu, 2002)²; and
- 3) Printing and paint thickness compensation (patent no. CN 103103814 A, 2013)³.

Offset printing and digital printing achieve high-fidelity replication of oil paintings visually, yet they are unable to replicate the feel of paintings. Screen printing cannot produce reproductions that are consistent with the originals given the unevenness and height of the paint. Moreover, paint thickness compensation in screen printing cannot achieve consistency with the originals in terms of stroke thickness, and its procedures are complicated.

Color representation and consistent stroke thickness with the originals are the main issues to be solved to obtain high-fidelity replications of oil paintings. Such issues can be addressed by 3D printing, in which a digital model file is used as a basis to print layer

by layer with powdered metal, plastic, or any other adhesive material⁴.

In conclusion, 3D digitalization technology is very important for 3D printing and high-fidelity reproductions of oil paintings.

2. Photogrammetry-based 3D reconstruction of oil paintings

The 3D reconstruction and digital representation of oil paintings mainly includes two aspects: 3D geometric information recovery of oil painting surface and color rendition of oil painting. Photogrammetry can acquire a digital 3D model of the surface geometrics of an oil painting, restore the color image and plane geometry of the painting in the form of orthophotomap, and implement the 3D digital representation of color in the painting.

2.1 Control grid and image capture

An original painting is shown in Fig. 2-1 and has stereoscopic undulating strokes for the petals.



Fig.2-1 Original painting.

A control grid is mainly designed to suppress measurement errors. A control grid plate used as the control plane to restore the painting, the interval of the control grid is 40 mm, and the grid contains 10 mm×10 mm square black boxes with a measurement accuracy of up to 0.1 mm. A standard light box with D65 illuminants is used to control the effect of ambient light. The oil painting is affixed flush to the control panel, as shown in Fig. 2-2.



Fig. 2-2 Control panel and measurement grid.

After the control grid is established, a Canon 5D II camera with a fixed focus lens is used to obtain a total of 35 sequence images. The focal length is set to 50 mm, and the shooting distance is 50 mm, as shown in Fig. 2-3.

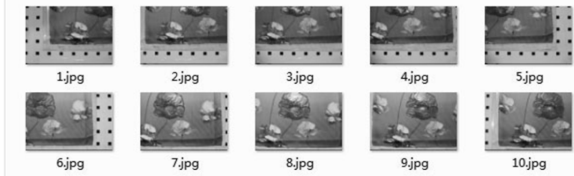


Fig. 2-3 Image sequence.

2.2 Analysis of photogrammetry triangulation

Collinearity equation is a condition equation that represents the image point, the center of projection, and the object point that should be located on a same straight line (Fig. 2-4).

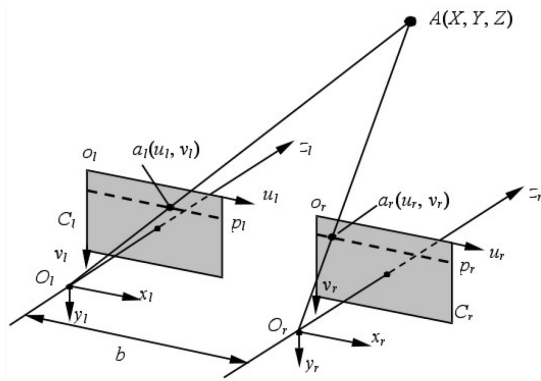


Fig. 2-4 Schematic of collinearity equations .

The coordinates of the object point can be used to solve when the known stereoscopic image corresponds to the orientation elements of two photos. Collinearity equations (Formula 2-1) are the most important analytic relations for photogrammetry, and two of them are plane equations. The intersecting line of the two corresponding planes is also the line where the image point, the center of projection, and the object point are located.

$$\begin{aligned} x - x_0 + \Delta x &= -f \frac{a_1(X - X_s) + b_1(Y - Y_s) + c_1(Z - Z_s)}{a_3(X - X_s) + b_3(Y - Y_s) + c_3(Z - Z_s)} \\ y - y_0 + \Delta y &= -f \frac{a_2(X - X_s) + b_2(Y - Y_s) + c_2(Z - Z_s)}{a_3(X - X_s) + b_3(Y - Y_s) + c_3(Z - Z_s)} \end{aligned} \quad (2-1)$$

where x, y respectively represent the image plane coordinates of the image point;

x_0, y_0, f represent the interior orientation elements of the image;

$\Delta x, \Delta y$ represent the correction values of system errors that are introduced by the coordinates of the image point;

X_s, Y_s, Z_s represent the object space coordinates of the position of the principal point of the camera when shooting;

X, Y, Z represent the object space coordinates of the object point;

a_i, b_i, c_i ($i=1, 2, 3$) represent the cosines of 3 exterior orientation elements of the image in 9 directions;

The interior orientation elements are obtained through camera calibration, as given in the following formula.

Radial distortion:

$$\begin{cases} x_u = x_d (1 + k_1 r^2) \\ y_u = y_d (1 + k_2 r^2) \end{cases} \quad (2-2)$$

k_1, k_2 represent the radial distortion parameters;

$r = \sqrt{x^2 + y^2}$ represent the polar radius of point to the

center of the imaging plane;

x_u, y_u represent the coordinates of x_d, y_d after calibration.

Decentering distortion:

$$\begin{cases} \delta_{x_d} = p_1 (3x_d^2 + y_d^2) + 2p_2 x_d y_d \\ \delta_{y_d} = p_2 (x_d^2 + 3y_d^2) + 2p_1 x_d y_d \end{cases} \quad (2-3)$$

x_d, y_d represent the coordinates of actual point;

p_1, p_2 represent the decentering distortion parameters.

The results seen as follow:

Table 2-1 Camera calibration data (unit: mm)

interior orientation elements	Distortion correction parameter					
Foc						
al-	x_0	y_0	k_1	k_2	p_1	p_2
Len						
53.0	0.00	0.04	2.402	5.553	6.068	4.729
279	817	196	e-000	e-017	e-008	e-007
1	7	4				

With the use of the control information available on the carrier platform and the acquired image for photogrammetry aerial triangulation by LENS PHOTO system automatically, six exterior orientation elements of each image are obtained, as shown in the following table:

Table 2-2 Exterior orientation elements of the image

linear elements(unit: mm)				angle elements(unit: degree)			
ID	Xs	Ys	Zs	ID	Phi	Omega	Kappa
1001	71.692	3.716	416.783	1001	8.59485	-3.6647	0.03352
1002	160.047	1.588	422.092	1002	8.68347	-0.60852	-0.12699
1003	221.435	1.557	423.021	1003	8.68914	1.52513	-0.06077
1004	271.147	1.802	421.971	1004	8.66924	3.25374	-0.06677
1005	339.917	1.549	417.466	1005	8.7875	5.74649	-0.03428
1006	342.58	74.244	423.867	1006	6.07698	5.82928	0.49472
1007	277.719	75.554	428.494	1007	6.04084	3.52869	0.70219
1008	230.162	78.806	430.056	1008	5.96971	1.85127	1.27968
1009	171.194	76.439	429.5	1009	6.10153	-0.21567	0.97029
1010	117.627	74.744	426.997	1010	6.19715	-2.12463	0.69722
1011	65.593	76.186	422.838	1011	6.1662	-3.94012	0.88023
1012	67.21	140.938	425.739	1012	3.60562	-3.77204	1.44554
1013	129.999	138.58	430.829	1013	3.9492	-1.68787	1.82183
1014	191.824	138.494	433.014	1014	3.97075	0.54517	1.95839
1015	249.514	139.733	432.674	1015	3.87468	2.60152	2.23126
1016	307.413	141.132	429.953	1016	3.80482	4.67805	2.60951
1017	357.936	141.452	425.576	1017	3.71014	6.30855	2.45238
1018	360.538	216.69	425.971	1018	1.5045	6.54967	3.14439
1019	310.385	221.351	430.215	1019	1.1811	4.80208	3.65246
1020	259.549	226.207	432.867	1020	0.97896	3.03272	4.3175
1021	207.521	227.01	433.643	1021	0.96299	1.20345	4.45399
1022	152.331	227.888	432.441	1022	0.98881	-0.75609	4.67229
1023	99.983	228.584	429.172	1023	1.10281	-2.56142	5.0965
1024	101.292	291.811	427.171	1024	-1.04216	-2.57623	3.68176
1025	97.981	293.917	426.829	1025	-1.11481	-2.64462	4.64974
1026	162.401	295.512	430.246	1026	-1.26319	-0.34378	4.90574
1027	226.246	296.514	430.739	1027	-1.32963	1.91508	5.28439
1028	289.258	297.375	428.67	1028	-1.34756	4.17922	5.87893
1029	343.392	298.821	424.443	1029	-1.27552	6.07808	5.42075
1030	343.504	356.699	419.706	1030	-3.29022	6.07678	5.34287
1031	272.988	353.335	424.943	1031	-3.2885	3.54492	4.34187
1032	213.031	350.936	426.391	1032	-3.1807	1.45214	3.79551
1033	155.814	344.691	426.086	1033	-2.94153	-0.64639	2.0446
1034	96.85	342.544	423.059	1034	-2.79908	-2.77061	1.75932
1035	51.148	345.778	418.649	1035	-2.86843	-4.31815	2.72225

Reconstructive accuracy analysis is created by LENS PHOTO system automatically, the root mean square of observation value and re-projection is 0.001330, the vertical accuracy of control points are shown in the following table:

Table 2-3 Vertical accuracy of control points

No.	$\Delta X(\text{mm})$	$\Delta Y(\text{mm})$	$\Delta Z(\text{mm})$
1	0.0031	0.0041	0.0036
2	0.0025	0.0032	0.0053
3	0.0021	0.0036	0.0027
4	0.0037	0.0032	0.0018
5	-0.0028	-0.0026	-0.0063
6	-0.0057	-0.0013	-0.0076

The 3D reconstruction results of the oil painting surface based on the interior and exterior orientation elements are shown in Fig. 2-5, 2-6.



Fig. 2-5 3D reconstruction results of the oil painting.

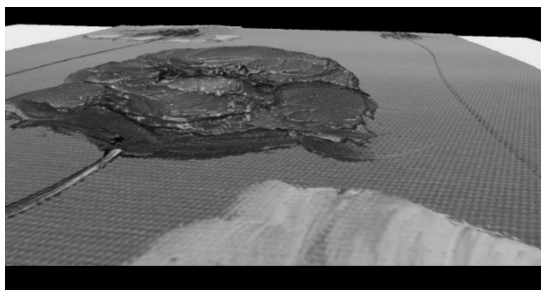


Fig. 2-6 Detail of 3D reconstruction

3. Conclusions

In this paper, a 3D digitization method for oil paintings is demonstrated experimentally. Digital photogrammetry is used for 3D modeling of oil paintings. Modeling results show that digital photogrammetry can effectively establish a colorful 3D model for oil paintings. The principle of the 3D model for oil painting surfaces is identical to that of DEM. This 3D digitization method for oil paintings compensates for the deficiencies of existing 2D digitization and reproduction methods and expands the applications of 3D printing. However, modeling accuracy and color rendition require further research.

4. Acknowledgement

This article is supported by The Guangdong Project of Construction of The Second Level Flagship Specialty(580301), Guangdong provincial Science and Technology Project (2017B090901064) and (2016070220045), Shenzhen Polytechnic Natural Science Research Project(601722K25022) and Hainan provincial Science and Technology Cooperation Project (KJHZ2015-23).

5. References

- [1] Yu Wenhua. Oil Painting Reproduction and Giclee[J]. Printing Technology, 2007, (10): 55-56.
- [2] Liu Anning. Prospects and Vision of the High-Fidelity Screen Printing Reproduction Market [J]. Printing World, 2002, (3): 16-17.
- [3] Liu Tianfu. A Oil Painting Reproduction with 3D Surface in China, CN 103103814 A[P/OL].
- [4] D. Dimitrov K.-Schreve, N.-de-Beer. Advances in three dimensional printing - state of the art and future perspectives[J]. Rapid Prototyping Journal, 2006, 12(3).
- [5] Ning Jingjing. Stereo Matching Algorithm Based on the Binocular Stereo Vision[D]. North University of China, 2012.

Author Biography

Chen Chen received his B.S. degree in Land Information System from the School of Geographical Sciences of the South China Normal University, Guangzhou, Guangdong. He received his M.S. degree in Land Information System in 2013 from the Institute of Resources and Environmental Engineering of Wuhan University, Wuhan, Hubei. He received his Ph.D. in Printing and Paper Engineering from South China University of Technology, Guangzhou, Guangdong in 2016. He is currently a postdoctoral fellow in Shenzhen Polytechnic, Shenzhen, Guangdong. His research interests cover the fields of 3D printing, reverse engineering and digital protection of cultural relics.

Wang Xiaochun received his B.S. degree in Environmental Sciences from the School of Anhui University Of Science & Technology, Huainan, Anhui in 2016. He is currently a master in South China University of Technology, Guangzhou, Guangdong. His research interests cover the fields of 3D printing and color management.

Chen Guangxue received his B.S. degree in Digital Printing from the School of Zhengzhou School For Surveying And Mapping, Zhengzhou, Henan. He received his M.S. degree in Digital Printing in 1995 from Northwest University, Xi'an, Shanxi. He received his Ph.D. in Digital Printing from Zhengzhou Information Engineering University, Zhengzhou, Henan in 2005. He is currently a professor in South China University of Technology, Guangzhou, Guangdong. His research interests cover the fields of digital printing, packaging and 3D printing.